CHEMMEDCHEM

DOI: 10.1002/cmdc.200900430

Semisynthetic Latrunculin Derivatives as Inhibitors of Metastatic Breast Cancer: Biological Evaluations, Preliminary Structure–Activity Relationship and Molecular Modeling Studies

Mohammad A. Khanfar,[a] Diaa T. A. Youssef,[b] and Khalid A. El Sayed*[a]

The microfilament cytoskeleton protein actin plays an important role in cell biology and affects cytokinesis, morphogenesis, and cell migration. These functions usually fail and become abnormal in cancer cells. The marine-derived macrolides latrunculins A and B, from the Red Sea sponge *Negombata magnifica*, are known to reversibly bind actin monomers, forming 1:1 stoichiometric complexes with G-actin, disrupting its polymerization. To identify novel therapeutic agents for effective treatment of metastatic breast cancer, several semisynthetic derivatives of latrunculin A with diverse steric, electrostatic, and hydrogen bond donor and acceptor properties were rationally prepared. Analogues were designed to modulate the binding affinity toward G-actin. Examples of these reactions are esterification, acetylation, and N-alkylation. Semisynthetic latrunculins were then tested for their ability to inhibit pyrene-conjugated actin polymerization, and subsequently assayed for their antiproliferative and anti-invasive properties against MCF7 and MDA-MB-231 cells using MTT and invasion assays, respectively.

Introduction

Actin is a cytoskeleton protein that forms versatile dynamic polymers, which can define cell polarity, organize cytoplasmic organelles, control cell shape, promote stable cell–cell and cell–matrix adhesions, and generate protrusive forces required for migration.[1] These functions usually fail and become abnormal in cancer cells.[1]

The marine-derived macrolides latrunculins A and B were first isolated by Kashman and co-workers from the Red Sea sponge *Negombata magnifi*ca.[2] Latrunculin A (**1**) was the first marine macrolide known to contain a 16-membered ring and the unique 2-thiazolidinone moiety connected by a tetrahydropyran (THP) ring.[2,3] Latrunculins A and B and their derivatives show antiangiogenic, antiproliferative, antimicrobial, and antimetastatic activities.[4,5] The most important biological effect of latrunculins is their ability to disrupt microfilament organization and to inhibit microfilament-mediated processes without affecting the organization of the microtubule system.[5–13] Latrunculin A reversibly binds cytoskeletal actin monomers, forming 1:1 stoichiometric complexes with G-actin, thereby disrupting its polymerization.[5–13] It has striking selectivity, rapid onset of action, and remarkable potency that exceed those of cytochalasin D by 1–2-fold.[9] Latrunculin A was also reported to decrease intraocular pressure and increase outflow facility without corneal effects in monkeys.[7,8] Latrunculin A also shows antiviral and antibacterial activities, inhibits the stress-activated MAP kinase (SAPK) pathway,[11] and suppresses hypoxia-induced factor (HIF-1) activation in breast cancer cells.[14] Therefore, latrunculin A is considered a potential lead, appropriate for further optimization studies.

Despite the remarkable physiological properties of latrunculins and their widespread use as biochemical tools, the present understanding of the structure–activity relationship (SAR) of these macrolides is fairly limited. Previous attempts at SAR studies were focused on the macrocyclic ring and semiquantitative testing.[15,16] An X-ray crystallographic structure of latrunculin A bound to actin monomers reveals that both the thiazolidinone and THP moieties are the key pharmacophores that direct the main binding and orientation of latrunculin A inside the ATP binding cleft.[12,13] Meanwhile, the macrocyclic ring is involved in hydrophobic interactions, and the hydrocarbon chain from C5 to C7 is exposed to the solvent, forming few contacts with actin and therefore playing a limited role in binding.[12] The detailed binding mode of **1** to G-actin was identified as having the following hydrogen bonding interactions: C1 carbonyl oxygen atom via water to Glu214 carboxyl group, C17 lactol hydroxy group to Arg210 NH (major binding), C17 pyran oxygen atom to Tyr69 hydroxy group, thiazolidinone NH to Asp157 carboxyl group, and thiazolidinone C20 carbonyl oxygen atom to Thr186 hydroxy group.[12,13] The only hydrogen bond donor (HBD) group was found to be the thiazolidinone NH, whereas the rest of binding functions act as hydrogen bond acceptors (HBA).[12,13] Therefore, efforts focused

[a] *M. A. Khanfar, Prof. K. A. El Sayed*
Department of Basic Pharmaceutical Sciences, College of Pharmacy
University of Louisiana at Monroe, Monroe, LA 71201 (USA)
Fax: (+1) 318-342-1737
E-mail: elsayed@ulm.edu

[b] *Prof. D. T. A. Youssef*
Department of Pharmacognosy, Faculty of Pharmacy
Suez Canal University, Ismailia 41522 (Egypt)

Supporting information for this article is available on the WWW under http://dx.doi.org/10.1002/cmdc.200900430.

on the optimization of the lactol hydroxy group and thiazolidinone NH of latrunculins should reflect better SAR insight.

Several C17 lactol hydroxy- and/or thiazolidinone NH-substituted latrunculin A derivatives **2**–**14** were produced by semisynthetic procedures (Scheme 1 and Table 1). Various aliphatic and aromatic substituents were used. Steric limitation, electrostatic, HBD and HBA properties were varied at these positions, and the biological activities of the resulting derivatives were tested. Because actin is essential for cellular proliferation and migration, these activities were quantified by cell proliferation (MTT) and cell invasion assays using MCF7 and MDA-MB-231 breast cancer cell lines, respectively.

Table 1. Structure of latrunculin A derivatives.

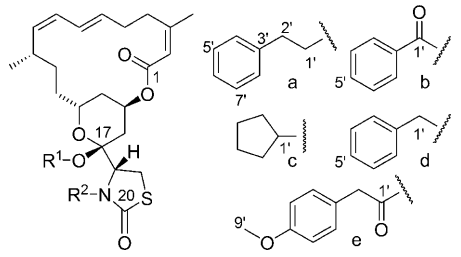

Compound	R^1	R^2
1	H	H
2	CH_3	H
3	a	H
4	b	H
5	CH_3	CH_3
6	CH_3	CH_2CH_3
7	CH_3	c
8	CH_3	$CH_2CH_2CH_2OH$
9	CH_3	d
10	CH_3	b
11	CH_3	e
12	H	CH_2CH_3
13	H	d
14	H	CH_2OH

Results and Discussion

Chemistry

Latrunculin A (**1**) was isolated from the Red Sea marine sponge *Negombata magnifica* and identified by detailed 1D and 2D NMR studies along with comparison with published data.[2] Reaction of **1** with methanol or phenylethanol in the presence of boron trifluoride diethyl etherate yielded the respective known 17-methoxy (compound **2**)[17] and new phenylethoxy (compound **3**) derivatives of **1** (Scheme 1). The configuration at C17 was maintained after acetalization of the C17 hydroxy group. This was confirmed by molecular modeling and NMR spectroscopy. The distance between proton H-18 and the C17 OCH_3 group in **2** was calculated by SYBYL to be 2.403 Å, which is in the range of NOE coupling. Proton H-18 and the C17 OCH_3 group showed a strong dipole–dipole coupling in NOESY experiments, confirming a similar β orientation. The ^{13}C NMR chemical shift of C17 in **2** (δ_C: 99.9 ppm) was almost identical to the reported value of the same carbon atom in 17β-methoxylatrunculin A (δ_C: 99.8 ppm).[17] Optical rotation values for compound **2** and 17β-methoxylatrunculin A were nearly identical.[17] Therefore, the β configuration at C17 was maintained in these semisynthetic latrunculin A derivatives.

High-resolution mass spectrometry (HRMS), ^1H NMR, and ^{13}C NMR data for compound **3** indicated the presence of the 17-*O*-phenylethyl side chain. The downfield shifts of the C17

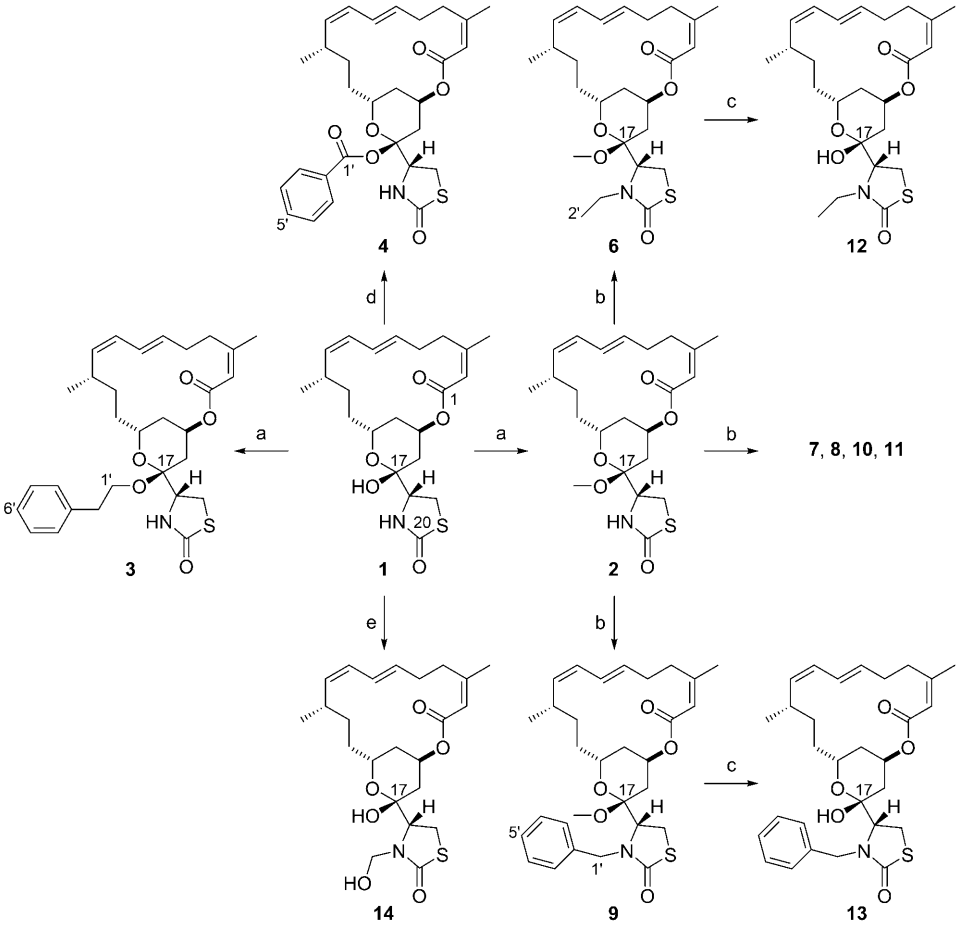

Scheme 1. Semisynthetic transformations of latrunculin A (**1**). Reagents and conditions: a) ROH, $Et_2O{\cdot}BF_3$, room temperature; b) 1. NaH, 0 °C, THF, 1 h, 2. RX, room temperature; c) $AcOH/H_2O/THF$ (3:1:1), 60 °C; d) benzoic anhydride, DMAP, $CHCl_3$ (anhyd), room temperature, 12 h; e) $CH_2O_{(aq)}$ (35%), EtOH, 24 h, 60 °C.

and H-18 signals in **3** (δ: +3.2 and 0.20 ppm, respectively) relative to that of the starting material **1** suggested possible etherification at C17.[2] The doublet of triplet of oxygenated methylene H_2-1′ (δ_H: 3.81, 3.51 ppm) showed COSY coupling with the benzylic H_2-2′ triplet (δ_H: 2.89 ppm). Protons H_2-1′ showed ^3J HMBC correlations with C17 and the aromatic quaternary carbon atom C3′ (δ_C: 138.3 ppm). Protons H_2-2′ showed ^3J HMBC correlations with the aromatic methine carbon atoms C4′/C8′ (δ_C: 128.9 ppm). Protons H-4′/H-8′ showed COSY couplings with protons H-5′/H-7′ and ^3J HMBC correlations with C6′ (δ_C: 126.7 ppm).

Compound **4** was prepared by treatment of **1** with benzoic anhydride in chloroform in the presence of 4-dimethylaminopyridine (DMAP) as a catalyst (Scheme 1). Analysis of ^{1}H and ^{13}C NMR data indicate benzoylation at C17. The HRMS data for **4** suggest the molecular formula $C_{29}H_{35}NO_6S$. The aromatic double doublet H-3′/H-7′ (δ_H: 7.69 ppm) showed COSY coupling with protons H-4′/H-6′ (δ_H: 7.42 ppm) and ^3J HMBC correlations with the carbonyl carbon atom C1′ (δ_C: 169.2 ppm). Protons H-4′/H-6′, in turn, showed COSY coupling with H-5′ (δ_H: 7.53 ppm) and ^3J HMBC correlations with the aromatic quaternary carbon C2′ (δ_C: 133.4 ppm). The downfield shift of H-18 (δ_H: 5.07, $>$+1.00 ppm) relative to that of the starting material **1** is possibly due to the anisotropic effect of the newly introduced C17-*O*-benzoyl functionality.

N-Substitution of **2** was carried out as shown in Scheme 1 using sodium hydride in anhydrous tetrahydrofuran at 0 °C and the corresponding alkyl and aryl halides to afford **5**–**11**.[17] The identity of **5** was confirmed by NMR spectroscopic analysis, which showed replacement of the thiazolidinone NH proton (δ_H: 5.80 ppm) with an *N*-methyl singlet (δ_H: 2.97 ppm and δ_C: 36.7 ppm); this is also supported by comparison with published data.[17] Similarly, the *N*-ethyl functionality in **6** was evident based on the COSY coupling between the downfield nitrogenated methylene H_2-1′ (δ_H: 3.71 and 3.35 ppm) with the methyl triplet H_3-2′ (δ_H: 1.17 ppm). Protons H_2-1′ also showed ^3J HMBC correlations with the carbonyl C20, connecting the new ethyl group with the thiazolidinone ring.

The HRMS data for compound **7** suggest an additional degree of unsaturation. Analysis of ^{1}H and ^{13}C NMR data further confirmed the new *N*-cyclopentyl moiety. The methine quintet H-1′ (δ_H: 3.88 ppm) showed ^3J HMBC correlations with the thiazolidinone carbonyl carbon atom (δ_C: 171.5 ppm) and the methylene carbon atoms C3′/C4′ (δ_C: 24.5 ppm). Protons H_2-3′/4′ showed COSY coupling with both H_2-2′/5′ protons, which, in turn, showed COSY coupling with H-1′.

Analysis of ^{1}H and ^{13}C NMR data for compound **8** suggested N-hydroxypropylation of the starting material **2**. The new methylene singlet H_2-1′ (δ_H: 3.55 ppm) showed a ^3J HMBC correlation with C29 carbonyl (δ_C: 170.2 ppm), connecting this moiety to the thiazolidinone ring. Protons H_2-1′ also showed a ^3J HMBC correlation with the oxygenated methylene carbon atom C3′ (δ_C: 59.2 ppm). The two chemically unequivalent H_2-3′ protons (δ_H: 3.76 and 3.58 ppm) showed COSY coupling with H_2-2′ (δ_H: 1.78 ppm), confirming the introduction of the new *N*-hydroxypropyl side chain.

High-resolution electrospray ionization mass spectrometry (HRESIMS) data for compound **9** suggest the molecular formula $C_{30}H_{39}NO_5S$, 12 degrees of unsaturation, and the N-benzylation of **2**. The downfield benzylic nitrogenate methylene protons H_2-1′ (δ_H: 5.11 and 4.35 ppm) showed a ^3J HMBC correlation with C20 carbonyl (δ_C: 170.2 ppm), connecting this moiety to the thiazolidinone ring. Protons H_2-1′ also showed a ^3J HMBC correlation with the symmetric aromatic methine carbons C3′/C7′ (δ_C: 128.4 ppm). Protons H-3′/H-7′ showed a ^3J HMBC correlation with the aromatic methine carbon C5′ (δ_C: 127.7 ppm) and COSY correlation with protons H-4′/H-6′ (δ_H: 7.34 ppm). The latter protons also show COSY correlation with H-5′ (δ_H: 7.31 ppm) and a ^3J HMBC correlation with the quaternary aromatic carbon C2′ (δ_C: 132.5 ppm).

The ^{1}H and ^{13}C NMR data for **10** were quite similar to those of compound **9**, with an *N*-benzoyl functionality instead of *N*-benzyl in **9**. The aromatic methine protons H-3′/H-7′ (δ_H: 7.72 ppm) showed a ^3J HMBC correlation with the carbonyl carbon C1′ (δ_C: 169.7 ppm). Notably, benzoylation of the lactol hydroxy group at C17 in **4** and the thiazolidinone NH in **10** resulted in a significant downfield shift of proton H-18 (δ: +1.22 and +1.49 ppm, respectively) relative to that of **1**, possibly due to the anisotropic effect of the benzene ring and the carbonyl group.

Reaction of **2** with *p*-methoxyphenylacetyl chloride afforded **11**, which was highly unstable in the reaction mixture; rapid degradation of the formed amide bond was observed. Therefore, the reaction time was shortened to five minutes after the addition of reagent. The HRESIMS data for compound **11** suggest the molecular formula $C_{32}H_{41}NO_7S$. The ^{1}H and ^{13}C NMR data for **11** suggest successful *N*-*p*-methoxyphenylacetylation. The methoxy singlet H_3-9′ (δ_H: 3.77 ppm) showed a ^3J HMBC correlation with the quaternary aromatic oxygenated carbon atom C6′ (δ_C: 159.8 ppm). The aromatic protons H-4′/H-8′ (δ_H: 7.21 ppm) showed ^3J HMBC correlations with C6′ and the benzylic methylene C2′ (δ_C: 42.3 ppm). They also show COSY coupling with protons H-5′/H-7′ (δ_H: 6.81 ppm). The proton singlet H_2-2′ (δ_H: 3.79 ppm) showed ^2J HMBC correlations with the carbonyl carbon C1′ (δ_C: 175.7 ppm) and the quaternary aromatic carbon C3′ (δ_C: 126.3 ppm). Proton H-18 (δ_H: 5.30 ppm) showed a ^3J HMBC correlation with C1′ carbonyl, connecting the new *p*-methoxyphenylacetyl moiety with the thiazolidinone ring.

To explore the importance of N-substitution on the pharmacological effect of the unsubstituted C17 lactol group, compounds **6** and **9** were demethylated by heating with aqueous acetic acid to afford **12** and **13**, respectively, with a free C17 lactol hydroxy functionality (Scheme 1).[17] Compounds **12** and **13** showed ^{1}H and ^{13}C NMR data identical to those of **6** and **9** with the replacement of C17 methoxy with a hydroxy group. The D_2O-exchangeable broad proton singlets at δ: 4.01 and 3.91 ppm were assigned as the new C17 hydroxy signals in **12** and **13**, respectively.

N-Hydroxymethyllatrunculin A (**14**) was prepared as previously reported to study the effect of extending the location of the only HBD in **1** (the thiazolidinone NH) by a methylene unit and its replacement with a primary alcohol group (Scheme 1).[17]

Biological activity

The cytoskeleton is composed of three distinct elements: actin microfilaments, microtubules, and intermediate filaments.[1,5,9–11] Microtubules form a polarized network, enabling the movement of organelles and proteins throughout the cell.[5,10] Intermediate filaments are rigid components that maintain the overall cell shape.[5,10] The actin cytoskeleton and other proteins involved in its regulation and function constitute more than 25% of the total cellular protein content.[1,5,9–11] Cytoskeletal elements coordinate and regulate cellular motility, adhesion, division, and exo- and endocytosis.[5,9–11] Actin filaments were found to be disrupted in malignant transformed cells.[1,5,9–11] Alteration of actin polymerization or its remodeling is important in regulating the morphology and phenotypic events of a malignant cell.[1,5,9–11] Actin alterations are progressive, and distinct actin remodeling profiles are correlated with various stages of cancer development and progression.[1,5,9–11] Compound **1** reversibly binds cytoskeletal actin monomers, forming a 1:1 complex with G-actin, thereby disrupting its polymerization.[5–13] Compound **1** has shown antiangiogenic, antiproliferative, antimicrobial, and antimigratory activities; it has been directly correlated with the amelioration of diseases in which the stability of cytoskeletal actin is intricately associated with the pathology.[1–6,10,14]

An actin polymerization kit was used to assess the direct actin binding activity of each analogue at two concentrations: 100 nM and 1 μM. This kit is based on the enhanced fluorescence of pyrene-conjugated actin that occurs during polymerization. The increase in fluorescence that results when pyrene–G-actin monomers assemble to form pyrene–F-actin can be used to follow polymerization as a function of time.[18,19] Table 2 lists the activities as the percentage of actin polymerization inhibition relative to the negative vehicle (DMSO) control along with calculated IC_{50} values. Figure 1 shows the time-dependent inhibition profiles of actin polymerization for compounds **1** and **3**. Compounds **3** and **14** were profoundly more active than the parent latrunculin A (**1**) in the inhibition of actin polymerization at both doses, whereas compounds **4**, **9**, **12**, and **13** were nearly equipotent to **1**. This specific binding assay proves that the antiproliferative and anti-invasive activities of latrunculin A derivatives are due to the disruption of actin polymerization, except in the case of compound **11**.

Table 2. Pyrene actin polymerization assay of latrunculin A derivatives.

Compound	Actin polymerization inhibition [%] 100 nM	1 μM	IC_{50} [nM][a]
1	30	73	284±72
2	6	21	9233±825
3	31	94	184±48
4	23	67	466±51
5	11	19	>10000
6	0	18	>10000
7	20	49	1049±271
8	0	21	8548±574
9	33	67	333±76
10	17	53	834±109
11	0	13	>10000
12	32	70	283±51
13	24	64	445±79
14	35	90	210±54

[a] IC_{50} values were determined from nonlinear dose–response curves using GraphPad Prism; values are the mean ±SEM; each experiment was conducted in triplicate.

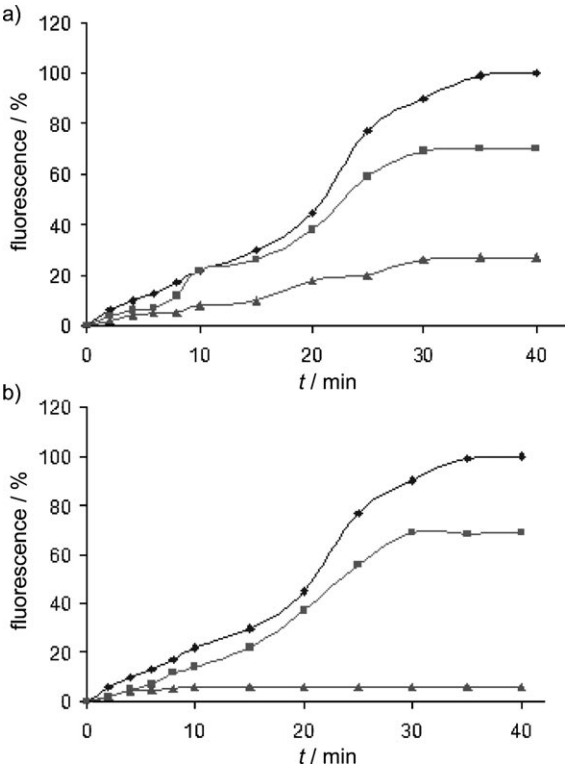

Figure 1. Time course for actin polymerization in the absence (◆) and presence of a) **1** and b) **3** at doses of 0.1 (■) and 1.0 μM (▲). Polymerization was monitored by an increase in fluorescence intensity.

The antiproliferative and anti-invasive activities of **1**–**14** were quantified using MTT and cell invasion assays, respectively. Latrunculin A (**1**) was used as a positive control in all biological assays because it is an established actin polymerization inhibitor and has documented cytotoxic, antiproliferative, and anti-invasive activities.[1,4–6,9–16] The 3-[4,5-dimethylthiazol-2-yl]-2,5-diphenyltetrazolium bromide (MTT) assay detects living cells in a quantitative colorimetric fashion, as it exploits the cells' ability to reduce MTT into an insoluble purple formazan dye.[20,21] This method is routinely used to assess a given compound's cytotoxicity and proliferation inhibitory activity. The antiproliferative activities of **1**–**14** were measured against two human mammary gland adenocarcinoma cell lines, MCF7 and MDA-MB-231, at five different concentrations: 0.1, 0.5, 1, 10, and 50 μM. The calculated IC_{50} values are listed in Table 3. While many of the prepared semisynthetic latrunculins retained activity, some of them were more active than the parent natural product **1**. Compounds **3** and **14** were more potent than **1** against both cell lines, with respective 4.8- and 4.0-fold increases in activity against MCF7, and notable cytotoxic effects at doses greater than 1 μM. Although MDA-MB-231 cells were more resistant than MCF7 against most derivatives, compound

Table 3. Antiproliferative activities of latrunculin A derivatives.

Compound	IC_{50} [μM][a] MCF7	MDA-MB-231
1	0.48 ± 0.04	4.19 ± 1.49
2	10.19 ± 1.72	23.42 ± 0.85
3	0.10 ± 0.07	2.71 ± 0.52
4	0.52 ± 0.14	5.05 ± 0.36
5	13.07 ± 3.69	19.93 ± 3.27
6	20.64 ± 2.77	> 50.0
7	5.30 ± 1.32	5.07 ± 0.72
8	19.20 ± 3.91	> 50.0
9	0.78 ± 0.24	6.82 ± 1.41
10	0.55 ± 0.091	4.48 ± 1.79
11	15.4 ± 1.21	26.17 ± 3.91
12	0.95 ± 0.28	7.19 ± 1.01
13	0.63 ± 0.02	2.72 ± 0.39
14	0.12 ± 0.01	2.99 ± 0.15

[a] IC_{50} values were determined from nonlinear dose–response curves using GraphPad Prism; values are the mean ± SEM; each experiment was conducted in triplicate.

14 retained potent activity against both cell lines. Although derivative **10** was less active than **1** in the invasion assay, this compound, along with **4** and **9**, was nearly equipotent to the parent natural product **1** in the proliferation assay.

The anti-invasive activities of **1**–**14** were measured using a 96-well basement membrane extract (BME) cell invasion assay against the highly metastatic MDA-MB-231 cells.[22,23] This assay employs a simplified Boyden chamber design with a polyethylene terephthalate membrane (8 μm pore size). Detection of cell invasion is quantified with calcein acetomethylester (AM).[22,23] Cells internalize calcein AM, and intracellular esterases cleave the AM moiety to generate free calcein. Free calcein fluoresces brightly, and this fluorescence is used to quantify the number of cells that have invaded across the BME.[22,23] The anti-invasive activities of **1**–**14** at three different concentrations are shown in Figure 2. To correlate the anti-invasive activities of latrunculin A derivatives with their actin-disrupting effect, **1**–**14** were tested at nontoxic concentrations. With the exception of compound **3**, the MTT assay results showed no or insignificant toxicity at concentrations of ≤ 1.0 μM for latrunculin derivatives over 72 h. Therefore, all compounds were tested at 0.1, 0.5, and 1.0 μM. Latrunculin **3** killed 17% of MDA-MB-231 cells at 1.0 μM, while the same concentration of **3** inhibited MDA-MB-231 cell invasion by 95%. This shows a clear distinction between the cytotoxic and anti-invasive activity levels. Therefore, the anti-invasive activities of **1**–**14** are attributed to the inhibition of actin polymerization and are not due to cell death.

Derivatives **3**, **11**, **13**, and **14** were 3.3-, 4.6-, 3.1-, and 2.1-fold more active than latrunculin A (**1**), respectively, at 0.5 μM. 17-*O*-Phenylethyllatrunculin A (**3**) was the most potent, with a concentration of 100 nM required to inhibit MDA-MB-231 cell invasion versus a dose of 1 μM for **1**. Upon the addition of **1**, **3**, and **14** to MDA-MB-231 cells in the upper assay chamber, rapid changes in cell morphology were observed, and actin filaments were disrupted, as characterized by remarkable cell deformity (data not shown). The actin cytoskeleton is dynamically remodeled during cell migration, and this reorganization produces the forces necessary for cell motility.[5,10,11] This suggests that the anti-invasive activities of **1**, **3**, and **14** are mediated through direct disruption of actin cytoskeleton remodeling. Interestingly, the second most active derivative, *N*-*p*-methoxyphenylacetyl-15-*O*-methyllatrunculin A (**11**) showed potent anti-invasive activity at 100 nM (Figure 2). This activity was nearly fourfold more active than that of **1** at the same concentration without antiproliferative, cytotoxic, or cell-shape-modifying activities. Furthermore, because it shows weak actin polymerization inhibition (Table 2), compound **11** has different target(s) other than the microfilament actin. Whereas compounds **4** and **12** are equipotent to compound **1** at concentrations of 1 and 0.5 μM, the rest were less active.

It has been reported that latrunculin A binds to actin monomers in the presence of ATP and acts by interfering with con-

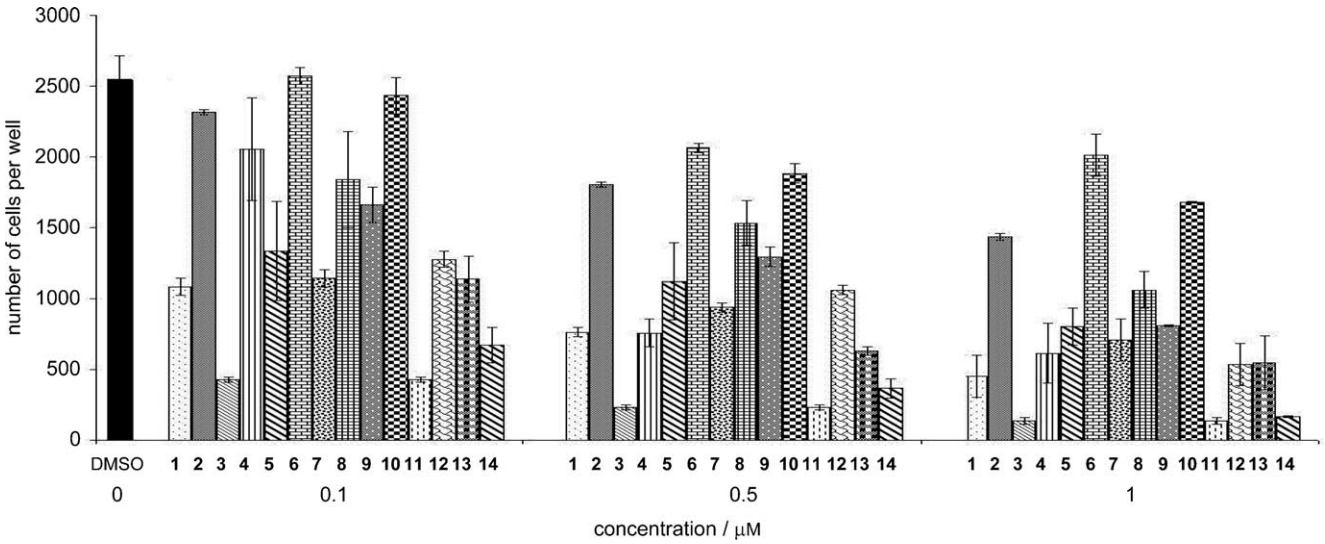

Figure 2. Anti-invasive activities of latrunculin derivatives **1**–**14** against MDA-MB-231 cells using a Cultrex® assay kit. Error bars indicate the SEM of $n = 3$ experiments per concentration.

formational changes that are necessary for polymerization.[12,13] Occupation of the latrunculin binding site clamps ATP in its buried site by preventing movement between subdomains II and IV.[12,13] Therefore, it is less likely that latrunculin A or its derivatives can act as ATP-competitive inhibitors.

Preliminary structure–activity relationships

X-ray crystallographic data revealed the binding site of latrunculin A is located above the actin nucleotide binding site in a cleft between subdomains II and IV.[12,13] The thiazolidinone and THP ring systems are the primary pharmacophores that direct the orientation and binding affinity, while the macrocyclic ring is mainly involved in hydrophobic interactions, with no contact with actin at the C5–C7 chain.[12,13] Furthermore, the bare macrocyclic system does not induce polymerization of F-actin at 10 μM concentration.[16] Therefore, the two accessible functional groups, C17 hydroxy and the thiazolidinone nitrogen atom, were used to investigate the steric limitations, electronic properties, and HBD and HBA characteristics at these positions to probe the chemical tolerance surrounding the binding-determinant amino acids Tyr69, Asp157, Thr186, Glu214, and Arg210.

Previously reported latrunculin derivatives were used as the basis by which to design new derivatives to get a better understanding of the SAR.[4,14–16] Our earlier results revealed the importance of both the thiazolidinone and THP ring systems in actin binding.[4,14] However, a clear SAR was not revealed. For example, it was shown that aliphatic substitution at the C17 lactol hydroxy group decreases activity,[4] unlike some aromatic substitutions, which increase activity.[14] N-Acetylation of the thiazolidinone nitrogen atom does not disrupt actin binding, although it has a strong interaction with Asp157 and is considered the only HBD pharmacophore in the molecule.[4] Therefore, the chemically accessible C17 lactol hydroxy and thiazolidinone NH groups were selected to probe the chemical space around these two critical pharmacophores.

Although the internal binding site of latrunculin A is compact, aromatic or aliphatic substitutions with defined steric and electronic properties will not change the binding orientation or the important interactions, as described below by simulated docking for each active derivative. Despite the fact that the C17 lactol hydroxy group acts as an HBA and not an HBD, the anti-invasive and antiproliferative activity of methylated derivative **2** was extensively suppressed despite the fact that the methoxy oxygen atom can still act as an HBA (Figure 2, Table 3). This result is consistent with those previously reported for 15-*O*-methyllatrunculin B.[4] In contrast, aromatic substitution of the thiazolidinone nitrogen atom restores actin binding activity, as is the case for compounds **9** and **10**, but not for **11**, in which the extra steric effect of the C9′ methoxy group weakens ligand binding. This outcome can be explained by MOLCAD visualization of the docked pose of **9** in the actin binding site (Figure 3). The benzyl moiety fills the pocket formed by Gly156, Gly182, and Arg210, and establishes a strong charge-transfer interaction between the π electron aromatic cloud of **9** and the positively charged guanidine group

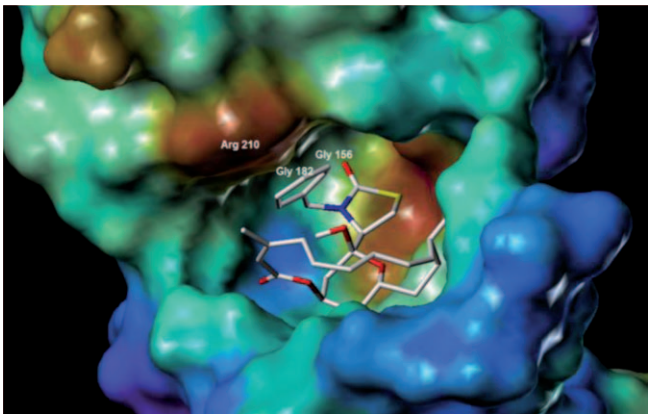

Figure 3. MOLCAD visualization of the electrostatic surface potential of the actin binding site with compound **9** docked using SurFlex-Dock program. Some non-interacting amino acids were omitted for clarity in viewing the important internal residues.

of Arg210 and possibly Arg206, while the acetyl moiety in **11** is too long to allow such interactions, given the added steric effect of the methoxy group. Because this interaction is absent in *N*-methyl and *N*-ethyl substituents of **2**, derivatives **5** and **6** were drastically less active both in the antiproliferation and anti-invasion assays. SurFlex-Dock software uses Hammerhead screens for the binding of flexible ligands to a protein binding site.[24,25] Ligand fragments are generated by breaking rotatable bonds and are then aligned onto the protomol probes. The highest-scoring fragmented poses are retained and proceed until the ligand is complete.[24,25] This docking procedure allows the *N*-benzyl substitution of **9** to be accommodated between the macrocyclic ring and Arg210 by rotating the thiazolidinone moiety outward by 2.6 Å and reallocating the macrocycle ring outward by 1.7 Å. Superimposition of the docked pose of **9** with the crystallographic structure of **1** (see Figure 6 below) shows that this shift in the thiazolidinone ring position does not disrupt the hydrogen bonding interaction with Thr186, but instead places the aromatic ring at an optimum distance near the guanidine moiety of Arg210 away from the interior compact area (Figure 3 and Figure 6).

Although analogue **11** was dramatically less active than **1** in the antiproliferation assay, it was quite potent in attenuating the metastasis of MDA-MB-231. This surprising observation can be explained by the potential activity of **11** on protein target(s) other than actin, as previously observed with other latrunculin derivatives.[14,15] It is evident that certain chemical changes in latrunculin A can ultimately change its molecular target.

N-Substitution of **1** with ethyl and benzyl groups preserves the potency of **1** with IC_{50} values of 0.63 and 0.95 μM for **13** and **12**, respectively, against MCF7 cells, whereas MDA-MB-231 cells are more resistant, with IC_{50} values of 2.72 for **13** and 7.19 μM for **12**. This result is consistent with the previously tested *N*-acetyllatrunculin B, which has potent antimigratory activity against murine brain metastatic melanoma cells (B16B15b).[4] On the other hand, the *N*-hydroxypropyl analogue **8** has significantly decreased activity for two reasons: 1) blocking the C17 hydroxy group with no aromatic replace-

ment effect as discussed above, and 2) the propyl chain is too long to allow hydrogen bonding interactions between the hydroxy group and the carboxylate of Asp157.

The most active derivative in actin binding, compound **3**, was docked into the active site of actin using SurFlex-Dock to understand its significant potency. The docked pose (Figure 4)

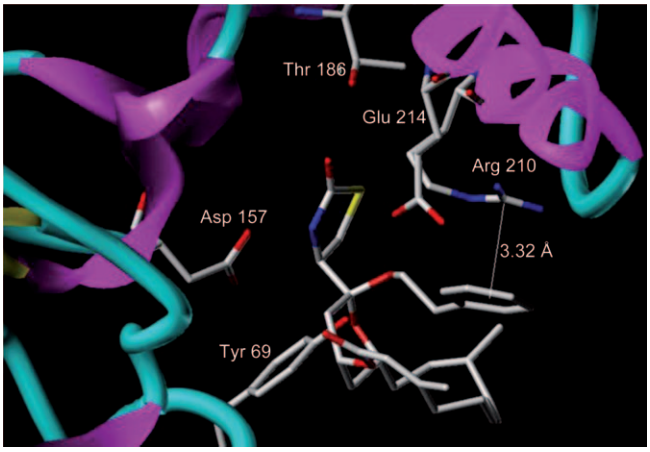

Figure 4. Detailed view of the docked structure of **3** with the corresponding interacting amino acids of the actin binding site.

shows optimum electrostatic interactions between the π electron cloud of the aromatic ring and the positively charged guanidine moiety of Arg210, and maintenance of the strong hydrogen bonding interactions with Tyr69, Asp157, Thr186, and Glu214. The calculated distance (using SYBYL 8.0) between the aromatic ring and the guanidine moiety is 3.32 Å, which is ideal for electrostatic interactions. This bulky phenylethyl moiety is accommodated between the macrocyclic ring, which is shifted outward and exposed more to the solvent (Figures 4 and 6), and Arg210 without inappropriate crash (see below) or conformational change in actin. In a previous study, 17-*O*-phenylcarbamoyllatrunculin A was observed to be fivefold more potent than **1** in invasion assays against PC-3M-CT+ cells.[14] The calculated length of the phenylcarbamoyl ($CONHC_6H_5$) moiety, from carbonyl carbon atom to the end of the aromatic ring, is 6.33 Å, which is very close to that determined for the phenylethyl moiety of **3** (6.12 Å). Therefore, a distance of 6.10–6.35 Å between aromatic substituents and the C17 hydroxy group can significantly improve the actin binding affinity of latrunculin A derivatives. It also appears that the C17 carbamate HBA/HBD feature does not play a direct role in the ATP binding site of actin.

In the proliferation assay, latrunculin derivative **14** shows improved activity over the parent latrunculin A (**1**) by 4- and 1.4-fold against MCF7 and MDA-MB-231 cells, respectively, and by 2.7-fold against MDA-MB-231 cells in the invasion assay at 1 μM. This pronounced activity of **14** can be partly explained by improved direct actin binding via the more accessible HBD *N*-hydroxyethyl group relative to the thiazolidinone NH in **1** (Figure 5). The proton of the primary hydroxy group in **14** can form a strong hydrogen bond with the carboxylate moiety of

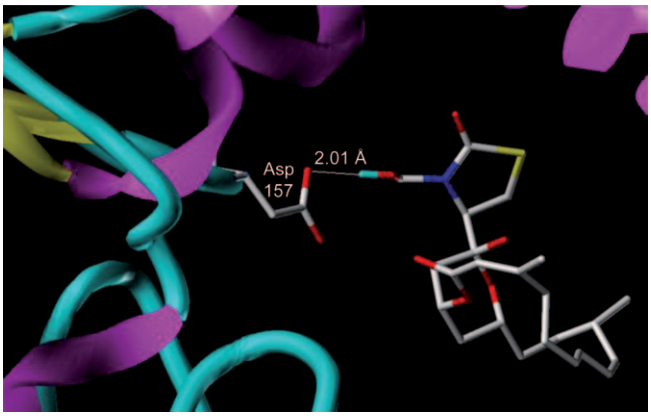

Figure 5. Hydrogen bonding interaction of docked compound **14** with the carboxylate moiety of Asp157 at optimal distance calculated by SYBYL 8.0.

Asp157 due to an optimal distance of 2.01 Å between the two functionalities (Figure 5), whereas this distance is 2.87 Å in the case of compound **1** as calculated by SYBYL 8.0 (Figure 6). Furthermore, the primary hydroxy group forms a more stable hydrogen bond than the amide nitrogen atom of the thiazolidinone moiety.

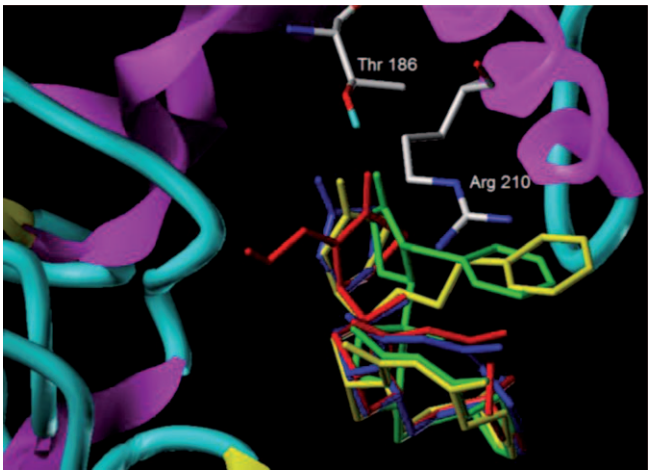

Figure 6. Superimposition of the crystallographic structures of **1** (blue) with the docked pose structures of **3** (yellow), **9** (green), and **14** (red).

One of the scoring functions that SurFlex-Dock calculates is crash. Crash is the degree of inappropriate penetration by the ligand into the protein and interpenetration (self-clash) between ligand atoms that are separated by rotatable bonds. Crash scores close to zero are favorable. Negative numbers indicate penetration.[24] All crash values were in the range of −0.11 to −0.87, which indicate appropriate penetration with no ligand–protein crash.

Conclusions

Actin is involved in numerous normal cellular activities and also plays a role in various pathological conditions. Owing to the high potency and cytotoxicity of latrunculin A (**1**), this

study is aimed at describing the structural features that can be altered to modulate the activity of **1**.

Latrunculin A is a potent and selective inhibitor of actin polymerization. To probe the chemical space around the binding-determinant moieties—the C17 hydroxy group and thiazolidinone nitrogen atom—they were substituted by various aromatic and aliphatic groups. It has been shown that the C17/C15 lactol hydroxy group is essential for actin binding affinity and therefore noticeably affects the antiproliferative and anti-invasive activities. Alkyl substitutions at the C17 hydroxy group remarkably diminish biological activity; this is in contrast to aromatic substitutions at the thiazolidinone nitrogen, which restore activity with notable increases in potency. The SAR study of latrunculins provides insight for optimizing their activities toward actin polymerization.

An optimum balance between moderate inhibition of actin polymerization and low cytotoxicity can improve the therapeutic index of semisynthetically modified latrunculins for future use in controlling cancer cell invasion and migration, decrease the intraocular pressure in glaucoma, and inhibit the formation of tau hyperphosphorylated structures in Alzheimer's disease. Indeed, meeting such a balance could improve the treatment of other diseases in which the stability of the actin cytoskeleton is intricately connected to the given pathology.

Experimental Section

General experimental procedures

Measurements of optical rotation were carried out on a Rudolph Research Analytical Autopol III polarimeter. IR spectra were recorded on a Varian 800 FTIR spectrophotometer. ^{1}H and ^{13}C NMR spectra were recorded in $CDCl_3$, with $(CH_3)_4Si$ as an internal standard, on a JEOL Eclipse NMR spectrometer operating at 400 MHz for ^{1}H NMR and 100 MHz for ^{13}C NMR. HREIMS experiments were conducted at the University of Michigan on a Micromass LCT spectrometer. Analytical HPLC analyses were performed on a Dionex® Summit II system using a Phenomenex Luna 250×4.6 mm reversed-phase C_{18} column, and isocratic elution (100% MeOH) with UV detection set at λ 235 nm to verify the purity of each latrunculin. Purities of $>98\%$ were established for latrunculins **1**–**14** except analogue **9**, which showed 91% purity. Thin-layer chromatographic analysis was carried out on precoated silica gel 60 F_{254} 500 μm TLC plates (EMD Chemicals), using the developing systems *n*-hexane/EtOAc (1:1) or $CHCl_3$/MeOH (9:1). For column chromatography, silica gel 60 (EMD Chemicals, 63–200 μm), fine silica gel 60 (EM Science, <63 μm), and C_{18} silica gel (Bakerbond, Octadecyl 40 μm) were used. For Sephadex LH-20 column chromatography, *n*-hexane/$CHCl_3$ (1:3), $CHCl_3$, and $CHCl_3$/MeOH (9:1) solvent systems were used.

Chemical syntheses

General procedure A

Acetalization of the C17 hydroxy group of latrunculin A: $Et_2O{\cdot}BF_3$ was added to a solution of **1** in ROH. The mixture was stirred for 12 h at room temperature and was then neutralized with an aqueous solution of 10% $NaHCO_3$. The solvent was evaporated, and the residue was extracted with $CHCl_3$ and dried over $MgSO_4$. The residue after solvent evaporation was subjected to column chromatography (silica gel 60).[17]

General procedure B

Alkylation of the thiazolidinone nitrogen atom: A solution of **2** in dry THF was gradually added to a suspension of NaH (60% dispersion in mineral oil) in dry THF at 0 °C. The mixture was then stirred for 1 h at 0 °C. Alkyl halide was added, and the mixture was stirred at room temperature until **2** was completely depleted. Et_2O and H_2O were then added, the two layers were separated, and the organic layer was dried over Na_2SO_4. Evaporation of the solvents afforded a residue which was subjected to column chromatography (silica gel 60).[17]

General procedure C

Demethylation of 17-*O*-methyllatrunculin A derivatives: A solution of 17-*O*-methyllatrunculin A analogue in AcOH/H_2O/THF (3:1:1) was stirred and heated at 60 °C. The reaction was monitored by TLC until complete depletion of the starting material (~0.5–1 h). The mixture was then cooled to room temperature, neutralized with an aqueous solution of 10% $NaHCO_3$, and Et_2O was then added. The upper organic layer was then washed with H_2O, dried over anhydrous Na_2SO_4, and evaporated under reduced pressure. The residue was subjected to column chromatography (silica gel 60).[17]

17-*O*-Methyllatrunculin A (2): Compound **2** was prepared according to procedure A from **1** (200 mg, 0.72 mmol), MeOH (5 mL), and $Et_2O{\cdot}BF_3$ (0.22 mL, 1.77 mmol). Elution with *n*-hexane/EtOAc (8:2) afforded **2** (144 mg, 72.0%).[17]

17-*O*-Phenylethyllatrunculin A (3): Compound **3** was synthesized according to general procedure A from **1** (15 mg, 0.036 mmol), phenylethanol (1 mL, 7.131 mmol), and $Et_2O{\cdot}BF_3$ (15 μL, 0.117 mmol). Elution with *n*-hexane/EtOAc (8:2) afforded **3** (5.5 mg, 36.7%): colorless oil, $[\alpha]_D^{25}=+34.5$ ($c=0.18$ in $CHCl_3$); ^{1}H NMR (400 MHz, $CDCl_3$): $\delta=5.41$ (1H, br s, H-2), 2.70 (1H, m, H-4a), 3.57 (1H, dt, $J=11.9$, 3.5 Hz, H-4b), 2.33 (1H, m, H-5), 5.87 (1H, dt, $J=15$ and 4.8 Hz, H-6), 6.43 (H1, dd, $J=15$ and 10.6 Hz, H-7), 6.08 (1H, dd, $J=10.8$ and 10.6 Hz, H-8), 5.01 (1H, dd, $J=10.6$ and 10.4 Hz, H-9), 2.81 (1H, m, H-10), 1.11 (1H, m, H-11a), 1.74 (1H, m, H-11b), 1.46 (2H, m, H-12), 4.24 (1H, m, H-13), 1.42 (1H, m, H-14a), 1.66 (1H, m, H-14b), 5.17 (1H, br t, $J=2.9$ Hz, H-15), 1.89 (1H, dd, $J=15.4$ and 4.4 Hz, H-16a), 2.15 (1H, m, H-16b), 4.05 (1H, dd, $J=7.3$ and 7.3 Hz, H-18), 3.07 (1H, dd, $J=11.4$ and 6.6 Hz, H-19a), 3.13 (1H, dd, $J=11.4$ and 6.6 Hz, H-19b), 1.91 (3H, s, H_3-21), 0.98 (3H, d, $J=6.2$ Hz, H_3-22), 3.51 (1H, dt, $J=8.8$ and 7.0 Hz, H-1′a), 3.81 (1H, dt, $J=8.8$ and 7.0 Hz, H-1′b), 2.89 (2H, t, $J=7.3$ Hz, H-2′), 7.17 (1H, dd, $J=8.4$ and 1.8 Hz, H-4′), 7.29 (1H, m, H-5′), 7.22 (1H, br d, $J=7.0$ Hz, H-6′), 7.29 (1H, m, H-7′), 7.17 (1H, dd, $J=8.4$ and 1.8 Hz, H-8′), 5.68 ppm (1H, s, NH); ^{13}C NMR (75 MHz, $CDCl_3$): $\delta=166.4$ (qC, C1), 118.2 (CH, C2), 158.1 (qC, C3), 30.7 (CH_2, C4), 31.6 (CH_2, C5), 132.3 (CH, C6), 124.3 (CH, C7), 127.4 (CH, C8), 135.8 (CH, C9), 29.8 (CH, C10), 32.2 (CH_2, C11), 31.2 (CH_2, C12), 63.5 (CH, C13), 35.3 (CH_2, C14), 67.0 (CH, C15), 29.8 (CH_2, C16), 100.1 (qC, C17), 57.1 (CH, C18), 27.9 (CH_2, C19), 175.2 (qC, C20), 21.8 (CH_3, C21), 25.3 (CH_3, C22), 61.6 (CH_2, C1′), 36.9 (CH_2, C2′), 138.3 (qC, C3′), 128.9 (CH, C4′), 128.6 (CH, C5′), 126.7 (CH, C6′), 128.6 (CH, C7′), 128.9 ppm (CH, 8′); IR (neat): $\tilde{\nu}_{max}=$ 3528, 3416, 2927, 2855, 1687, 1455, 1132, 1090, 1020, 1984 cm^{-1}; HRMS-ESI: *m/z* $[M+Na]^+$ calcd for $C_{30}H_{39}NO_5SNa$: 548.2447, found: 548.2463.

17-*O*-Benzoyllatrunculin A (4): A solution of **1** (20 mg, 0.047) in anhydrous $CHCl_3$ (3 mL) was stirred with benzoic anhydride (11 mg, 0.050 mmol) and a catalytic amount of DMAP for 12 h at room temperature. The reaction mixture was neutralized with a solution of $NaHCO_3$. The organic layer was washed with H_2O (2×5 mL), dried over anhydrous Na_2SO_4, and evaporated under reduced pressure. The reaction residue was subjected to chromatography (silica gel 60) using isocratic *n*-hexane/EtOAc (9:1) to afford **4** (4.7 mg, 23.5%): colorless oil, $[\alpha]_D^{25} = +47.1$ ($c = 0.25$ in $CHCl_3$); ^{1}H NMR (400 MHz, $CDCl_3$): $\delta = 5.62$ (1H, brs, H-2), 2.36 (1H, dt, $J = 13.2$ and 7.3 Hz, H-4a), 3.02 (1H, dt, $J = 13.2$ and 7.32 Hz, H-4b), 2.22 (2H, dt, $J = 10.8$ and 6.2 Hz, H-5), 5.67 (1H, dt, $J = 15.4$ and 6.2 Hz, H-6), 6.20 (1H, dd, $J = 15.4$ and 10.6 Hz, H-7), 5.94 (1H, dd, $J = 11.0$ and 11.0 Hz, H-8), 4.89 (1H, dd, $J = 10.6$ and 10.6 Hz, H-9), 2.50 (1H, m, H-10), 1.01 (1H, m, H-11a), 1.70 (1H, m, H-11b), 1.48 (2H, m, H-12), 3.92 (1H, m, H-13), 1.01 (1H, m, H-14a), 1.69 (1H, m, H-14b), 5.19 (1H, t, $J = 4.0$ Hz, H-15), 1.63 (1H, m, H-16a), 1.81 (1H, m, H-16b), 5.07 (1H, dd, $J = 7.0$ and 7.0 Hz, H-18), 3.43 (1H, dd, $J = 11.0$ and 6.6 Hz, H-19a), 3.53 (1H, dd, $J = 11.0$ and 6.6 Hz, H-19b), 1.88 (3H, s, H_3-21), 0.66 (3H, d, $J = 6.2$ Hz, H_3-22), 7.69 (1H, dd, $J = 8.0$ and 1.5 Hz, H-3′), 7.42 (1H, dd, $J = 8.0$ and 7.4 Hz, H-4′), 7.53 (1H, dd, $J = 7.4$ and 1.5 Hz, H-5′), 7.42 (1H, dd, $J = 8.0$ and 7.4 Hz, H-6′), 7.69 (1H, dd, $J = 8.0$ and 1.5 Hz, H-7′), 5.61 ppm (1H, s, NH); ^{13}C NMR (75 MHz, $CDCl_3$): $\delta = 166.6$ (qC, C1), 118.3 (CH, C2), 157.1 (qC, C3), 33.2 (CH_2, C4), 30.7 (CH_2, C5), 132.5 (CH, C6), 126.2 (CH, C7), 127.8 (CH, C8), 135.9 (CH, C9), 29.3 (CH, C10), 31.5 (CH_2, C11), 30.9 (CH_2, C12), 64.3 (CH, C13), 35.0 (CH_2, C14), 71.0 (CH, C15), 35.7 (CH_2, C16), 97.7 (qC, C17), 61.2 (CH, C18), 29.7 (CH_2, C19), 172.1 (qC, C20), 24.8 (CH_3, C21), 21.5 (CH_3, C22), 169.2 (qC, C1′), 133.4 (qC, C2′), 129.4 (CH, C3′), 128.2 (CH, C4′), 133.1 (CH, C5′), 128.2 (CH, C6′), 129.4 ppm (CH, C7′); IR (neat): $\tilde{\nu}_{max} = 3694$, 3522, 3202, 2928, 2956, 1690, 1602, 1451, 1378, 1281, 1153, 1118, 971 cm^{-1}; HRMS-ESI: *m/z* $[M+Na]^+$ calcd for $C_{29}H_{35}NO_6SNa$: 548.2083, found: 548.2087.

17-*O*-Methyl-*N*-methyllatrunculin A (5): Compound **5** was prepared according to general procedure B using **2** as starting material (10 mg, 0.022 mmol) in THF (1 mL), NaH (2 mg, 0.041 mmol) in THF (1 mL), and MeI (0.1 mL, 1.600 mmol). Elution with *n*-hexane/EtOAc (8:2) afforded **5** (7.1 mg, 70.1%).[17]

17-*O*-Methyl-*N*-ethyllatrunculin A (6): Compound **6** was prepared according to general procedure B using **2** as starting material (10 mg, 0.022 mmol) in THF (1 mL), NaH (2 mg, 0.041 mmol) in THF (1 mL), and EtI (0.1 mL, 1.147 mmol). Elution with *n*-hexane/EtOAc (8:2) afforded **6** (7.6 mg, 70.6%): colorless oil, $[\alpha]_D^{25} = +33.7$; ($c = 1.3$ in $CHCl_3$); ^{1}H NMR (400 MHz, $CDCl_3$): $\delta = 5.63$ (1H, brs, H-2), 2.61 (1H, m, H-4a), 2.89 (1H, m, H-4b), 2.25 (2H, m, H-5), 5.78 (1H, dt, $J = 15.4$ and 4.0 Hz, H-6, 6.37 (1H, dd, $J = 15.4$ and 11.0 Hz, H-7), 6.04 (1H, dd, $J = 10.9$ and 10.6 Hz, H-8), 4.99 (1H, dd, $J = 10.6$ and 10.6 Hz, H-9), 2.84 (1H, m, H-10), 1.11 (1H, m, H-11a), 1.76 (1H, m, H-11b), 1.46 (2H, m, H-12), 4.16 (1H, m, H-13), 1.07 (1H, m, H-14a), 1.72 (1H, m, H-14b), 5.14 (1H, brt, $J = 4.0$ Hz, H-15), 1.79 (dd, $J = 15.4$ and 4.4 Hz, H-16a), 2.13 (1H, m, H-16b), 4.03 (1H, dd, $J = 9.9$ and 3.0 Hz, H-18), 3.25 (1H, dd, $J = 11.7$ and 3.0 Hz, H-19a), 3.35 (1H, m, H-19b), 1.91 (3H, brs, H_3-21), 1.02 (3H, d, $J = 6.24$ Hz, H_3-22), 3.35 (1H, dq, $J = 17.4$, 7.0 Hz, H-1′a), 3.71 (1H, dq, $J = 17.4$ and 7.0 Hz, H-1′b), 1.17 (3H, t, $J = 7.0$ Hz, H-2′), 3.33 ppm (3H, s, O-CH_3); ^{13}C NMR (75 MHz, $CDCl_3$): $\delta = 167.3$ (qC, C1), 118.5 (CH, C2), 158.5 (qC, C3), 32.5 (CH_2, C4), 30.7 (CH_2, C5), 132.3 (CH, C6), 125.0 (CH, C7), 127.8 (CH, C8), 135.6 (CH, C9), 29.4 (CH, C10), 31.4 (CH_2, C11), 31.3 (CH_2, C12), 63.2 (CH, C13), 35.1 (CH_2, C14), 66.7 (CH, C15), 35.2 (CH_2, C16), 101.2 (qC, C17), 60.6 (CH, C18), 25.5 (CH_2, C19), 173.6 (qC, C20), 25.1 (CH_3, C21), 21.8 (CH3, C22), 40.4 (CH_2, C1′), 29.7 (CH_3, C2′), 47.6 ppm (CH_3, O-CH_3); IR (neat): $\tilde{\nu}_{max} = 3693$, 3601, 2957, 2924, 1681, 1604, 1282, 1163 cm^{-1}; HRMS-ESI: *m/z* $[M+Na]^+$ calcd for $C_{25}H_{37}NO_5SNa$: 486.2290, found: 486.2281.

17-*O*-Methyl-*N*-cyclopentanelatrunculin A (7): Compound **7** was prepared according to general procedure B starting with **2** (10 mg, 0.022 mmol) in THF (1 mL), NaH (2 mg, 0.041 mmol) in THF (1 mL) and iodocyclopentane (0.1 mL, 0.867 mmol). Elution with *n*-hexane/EtOAc (8:2) afforded **7** (7.6 mg, 70.6%): colorless oil, $[\alpha]_D^{25} = +53.6$ ($c = 0.63$ in $CHCl_3$); ^{1}H NMR (400 MHz, $CDCl_3$): $\delta = 5.64$ (1H, brs, H-2), 1.41 (2H, m, H-4), 2.28 (2H, m, H-5), 5.80 (1H, dt, $J = 15.4$ and 3.6 Hz, H-6), 6.37 (1H, dd, $J = 15.4$ and 11.0 Hz, H-7), 6.04 (1H, dd, $J = 11.0$ and 10.6 Hz, H-8), 4.99 (1H, dd, $J = 10.6$ and 10.6 Hz, H-9), 2.83 (1H, m, H-10), 1.13 (1H, m, H-11a), 1.50 (1H, m, H-11b), 0.91 (1H, m, H-12a), 1.61 (1H, m, H-12b), 4.16 (1H, m, H-13), 1.41 (1H, m, H-14a), 1.61 (1H, m, H-14b), 5.16 (1H, brt, $J = 3.0$ Hz, H-15), 1.75 (1H, m, H-16a), 1.86 (1H, m, H-16b), 3.96 (1H, dd, $J = 9.5$ Hz, H-18), 3.42 (1H, m, H-19a), 3.47 (1H, dd, $J = 9.9$ and 6.6 Hz, H-19b), 1.91 (3H, s, H_3-21), 1.02 (1H, d, $J = 6.2$ Hz, H_3-22), 3.88 (1H, t, $J = 8.8$ Hz, H-1′), 2.14 (2H, m, H-2′), 1.81 (2H, m, H-3′), 2.05 (2H, m, H-4′), 1.81 (2H, m, H-5′), 3.28 ppm (3H, s, O-CH_3); ^{13}C NMR (75 MHz, $CDCl_3$): $\delta = 166.5$ (qC, C1), 118.5 (CH, C2), 157.7 (qC, C3), 31.3 (CH_2, C4), 28.6 (CH_2, C5), 132.4 (CH, C6), 125.0 (CH, C7), 127.8 (CH, C8), 135.6 (CH, C9), 29.8 (CH, C10), 30.8 (CH_2, C11), 29.5 (CH_2, C12), 63.9 (CH, C13), 35.0 (CH_2, C14), 66.7 (CH, C15), 32.4 (CH_2, C16), 101.6 (qC, C17), 63.1 (CH, C18), 26.2 (CH_2, C19), 171.7 (qC, C20), 25.1 (CH_3, C21), 21.8 (CH_3, C22), 60.7 (CH, C1′), 29.9 (CH_2, C2′), 24.5 (CH_2, C3′), 24.5 (CH_2, C4′), 29.9 (CH_2, C5′), 47.5 ppm (CH_3, O-CH_3); IR (neat): $\tilde{\nu}_{max} = 3696$, 3672, 2928, 2855, 1685, 1602, 1290 cm^{-1}; HRMS-ESI: *m/z* $[M+Na]^+$ calcd for $C_{28}H_{41}NO_5SNa$: 526.2603, found: 526.2603.

17-*O*-Methyl-*N*-(3′-hydroxypropyl)latrunculin A (8): Compound **8** was prepared according to general procedure B from **2** (10 mg, 0.022 mmol) in THF (1 mL), NaH (2 mg, 0.041 mmol) in THF (1 mL), and 3-iodo-1-propanol (0.1 mL, 1.043 mmol). Elution with *n*-hexane/EtOAc (8:2) afforded **8** (4.6 mg, 40.6%): colorless oil, $[\alpha]_D^{25} = +53.6$ ($c = 0.83$ in $CHCl_3$); ^{1}H NMR (400 MHz, $CDCl_3$): $\delta = 5.64$ (1H, s, H-2), 2.24 (2H, m, H-4), 2.25 (2H, m, H-5), 5.79 (1H, dt, $J = 5.4$ and 5.5 Hz, H-6), 6.39 (1H, dd, $J = 5.0$ and 11.0 Hz, H-7), 6.04 (1H, dd, $J = 10.7$ and 10.6 Hz, H-8), 5.01 (1H, dd, $J = 10.6$ and 10.6 Hz, H-9), 2.84 (1H, m, H-10), 1.09 (1H, m, H-11a), 1.65 (1H, m, H-11b), 1.43 (2H, m, H-12), 4.17 (1H, m, H-13), 1.46 (1H, m, H-14a), 1.77 (1H, m, H-14b), 5.15 (1H, brt, $J = 3.0$ Hz, H-15), 1.81 (1H, m, H-16a), 2.01 (1H, m, H-16b), 4.01 (1H, dd, $J = 9.9$ and 4.0 Hz, H-18), 3.27 (1H, dd $J = 12.8$ and 4.5 Hz, H-19a), 3.37 (1H, m, H-19b), 1.91 (3H, s, H_3-21), 1.01 (3H, d, $J = 6.6$ Hz, H_3-22), 3.55 (2H, m, H-1′), 1.78 (2H, m, H-2′), 3.58 (1H, m, H-3′a), 3.76 (1H, dt, $J = 8.1$ and 5.8 Hz, H-3′b), 3.31 (3H, s, O-CH_3), 5.64 ppm (s, OH); ^{13}C NMR (75 MHz, $CDCl_3$): $\delta =$ 166.3,(qC, C1), 118.3 (CH, C2), 154.2 (qC, C3), 30.2 (CH_2, C4), 29.8 (CH_2, C5), 132.3 (CH, C6), 124.8 (CH, C7), 127.9 (CH, C8), 153.6 (CH, C9), 29.7 (CH, C10), 31.4 (CH_2, C11), 31.2 (CH_2, C12), 63.3 (CH, C13), 35.2 (CH_2, C14), 66.5 (CH, C15), 32.4 (CH_2, C16), 101.0 (qC, C17), 61.4 (CH, C18), 29.4 (CH_2, C19), 170.2 (qC, C20), 25.2 (CH_3, C21), 21.8 (CH_3, C22), 41.8 (CH_2, C1′), 30.8 (CH_2, C2′), 59.2 (CH_2, C3′), 47.5 ppm (CH_3, O-CH_3); IR (neat): $\tilde{\nu}_{max} = 3694$, 3601, 3505, 2929, 2857, 2360, 1671, 1602, 1456, 1291, 1127, 1089 cm^{-1}; HRMS-ESI: *m/z* $[M+Na]^+$ calcd for $C_{26}H_{39}NO_6SNa$: 516.2396, found: 516.2388.

17-*O*-Methyl-*N*-benzyllatrunculin A (9): Compound **9** was prepared according to general procedure B using **2** as starting substrate (15 mg, 0.033 mmol) in THF (1 mL), NaH (2 mg, 0.041 mmol) in THF (1 mL), and benzyl chloride (0.1 mL, 0.866 mmol). Elution with *n*-hexane/EtOAc (9:1) afforded **9** (11.3 mg, 75.3%): colorless oil, $[\alpha]_D^{25} = +28.5$ ($c = 0.48$ in $CHCl_3$); ^{1}H NMR (400 MHz, $CDCl_3$): $\delta =$ 5.63 (1H, brs, H-2), 1.91 (1H, m, H-4a), 3.45 (1H, dt, $J = 13.6$ and 11.0 Hz, H-4b), 2.26 (2H, m, H-5), 5.82 (1H, dt, $J = 13.0$ and 5.1 Hz,

H-6), 6.35 (1H, dd, $J=15.4$ and 11.0 Hz, H-7), 6.04 (1H, dd, $J=10.8$ and 10.6 Hz, H-8), 5.01 (1H, dd, $J=10.6$ and 11.4 Hz, H-9), 2.80 (1H, m, H-10), 0.89 (1H, m, H-11a), 1.67 (1H, m, H-11b), 1.42 (1H, m, H-12a), 1.61 (1H, m, H-12b), 4.19 (1H, m, H-13), 1.38 (1H, m, H-14a), 1.88 (1H, m, H-14b), 5.15 (1H, brt, $J=3.0$ Hz, H-15), 1.51 (1H, m, H-16a), 1.95 (1H, m, H-16b), 3.82 (1H, dd, $J=9.2$ and 2.9 Hz, H-18), 3.23 (1H, dd, $J=15.0$ and 2.6 Hz, H19a), 3.28 (1H, dd, $J=15.0$ and 3.0 Hz, H-19b), 1.90 (3H, s, H_3-21), 1.01 (3H, d, $J=6.2$ Hz, H_3-22), 4.35 (1H, d, $J=14.6$ Hz, H-1′a), 5.11 (1H, d, $J=14.6$ Hz, H-1′b), 7.23 (1H, dd, $J=8.4$ and 1.4 Hz, H-3′), 7.34, (1H, dd, $J=7.3$ and 1.4 Hz, H-4′), 7.31 (1H, dd, $J=8.4$ and 7.3 Hz, H-5′), 7.34 (1H, dd, $J=7.3$ and 1.4 Hz, H-6′), 7.23 (1H, dd, $J=8.4$ and 1.4 Hz, H-7′), 3.17 ppm (3H, s, O-CH_3); ^{13}C NMR (75 MHz, $CDCl_3$): $\delta=166.5$ (qC, C1), 118.4 (CH, C2), 157.8 (qC, C3), 31.4 (CH_2, C4), 29.8 (CH_2, C5), 132.4 (CH, C6), 124.9 (CH, C7), 127.9 (CH, C8), 135.6 (CH, C9), 29.7 (CH, C10), 30.7 (CH_2, C11), 30.4 (CH_2, C12), 63.4 (CH, C13), 35.2 (CH_2, C14), 66.9 (CH, C15), 32.5 (CH_2, C16), 101.7 (qC, C17), 59.7 (CH, C18), 25.5 (CH_2, C19), 173.4 (qC, C20), 25.2 (CH_3, C21), 21.8 (CH_3, C22), 48.3 (CH_2, C1′), 132.5 (qC, C2′), 128.4 (CH, C3′), 128.8 (CH, C4′), 127.7 (CH, C5′), 128.8 (CH, C6′), 128.4 (CH, C7′), 47.6 ppm (CH_3, O-CH_3); IR (neat): $\tilde{\nu}_{max}=3523$, 3371, 2897–2816, 1731, 1744, 1544, 1344, 1354 cm^{-1}; HRMS-ESI: m/z $[M+Na]^+$ calcd for $C_{30}H_{39}NO_5SNa$: 548.2447, found: 548.2443.

17-*O*-Methyl-*N*-benzoyllatrunculin A (10): Compound **10** was prepared according to general procedure B using **2** as starting substrate (10 mg, 0.022 mmol) in THF (1 mL), NaH (2 mg, 0.041 mmol) in THF (1 mL), and benzoyl chloride (0.1 mL, 0.866 mmol). Elution with *n*-hexane/EtOAc (8:2) afforded **10** (5.2 mg, 52.0%): colorless oil, $[\alpha]_D^{25}=+42.7$ ($c=0.15$ in $CHCl_3$); ^{1}H NMR (400 MHz, $CDCl_3$): $\delta=$ 5.65 (1H, brs, H-2), 2.26 (1H, dt, $J=13.2$ and 7.3 Hz, H-4a), 3.48 (1H, dt, $J=13.3$ and 11.0 Hz, H-4b), 2.25 (2H, m, H-5), 5.76 (1H, dt, $J=14.6$ and 6.2 Hz, H-6), 6.34 (1H, dd, $J=14.6$ and 11.7 Hz, H-7), 5.99 (1H, dd, $J=11.0$ and 10.8 Hz, H-8), 4.89 (1H, dd, $J=11.0$ and 10.8 Hz, H-9), 2.71 (1H, m, H-10), 0.77 (1H, m, H-11a), 1.13 (1H, m, H-11b), 1.60 (2H, m, H-12), 4.05 (2H, m, H-13), 1.33 (1H, m, H-14a), 1.63 (1H, m, H-14b), 5.25 (1H, brt, $J=3.3$ Hz, H-15), 2.20 (1H, m, H-16a), 3.42 (1H, m, H-16b), 5.34 (1H, dd, $J=9.9$ and 1.4 Hz, H-18), 3.28 (1H, dd, $J=11.7$ and 1.4 Hz, H-19a), 3.60 (1H, dd, $J=11.7$ and 9.9 Hz, H-19b), 1.92 (3H, s, H_3-21), 0.95 (3H, d, $J=6.6$ Hz, H_3-22), 7.72 (1H, dd, $J=8.4$ and 1.5 Hz, H-3′), 7.42 (1H, brd, $J=7.3$ Hz, H-4′), 7.54 (1H, dd, $J=7.3$ and 1.5 Hz, H-5′), 7.42 (1H, brd, $J=7.3$ Hz, H-6′), 7.72 (1H, dd, $J=8.4$ and 1.5 Hz, H-7′), 3.35 ppm (3H, s, O-CH_3); ^{13}C NMR (75 MHz, $CDCl_3$): $\delta=166.5$ (qC, C1), 118.3 (CH, C2), 157.9 (qC, C3), 32.1 (CH_2, C4), 30.1 (CH_2, C5), 131.9 (CH, C6), 125.2 (CH, C7), 127.3 (CH, C8), 136.2 (CH, C9), 29.8 (CH, C10), 30.8 (CH_2, C11), 30.7 (CH_2, C12), 63.2 (CH_2, C13), 35.1 (CH_2, C14), 66.7 (CH, C15), 32.2 (CH_2, C16), 100.0 (CH, C17), 58.2 (CH, C18), 28.9 (CH_2, C19), 171.9 (qC, C20), 25.2 (CH_3, C21), 21.8 (CH_3, C22), 169.7 (qC, C1′), 133.8 (qC, C2′), 129.9 (CH, C3′), 133.2 (CH, C4′), 128.1 (CH, C5′), 133.2 (CH, C6′), 129.9 (CH, C7′), 48.2 ppm (CH_3, O-CH_3); IR (neat): $\tilde{\nu}_{max}=3693$, 3531, 2928, 2856, 2356, 1684, 1453, 1351, 1278, 1149 cm^{-1}; HRMS-ESI: m/z $[M+Na]^+$ calcd for $C_{30}H_{37}NO_6SNa$: 562.2239, found: 562.2234.

17-*O*-Methyl-*N*-(7′-methoxyphenylacetyl)latrunculin A (11): Compound **11** was prepared according to general procedure B from **2** (10 mg, 0.022 mmol) in THF (1 mL), NaH (2 mg, 0.041 mmol) in THF (1 mL), and *p*-methoxyphenylacetyl chloride (0.1 mL, 0.636 mmol). Elution with *n*-hexane/EtOAc (8:2) afforded **11** (2.2 mg, 22.0%): colorless oil, $[\alpha]_D^{25}=+63.6$ ($c=0.1$ in $CHCl_3$); ^{1}H NMR (400 MHz, $CDCl_3$): $\delta=5.61$ (1H, brs, H-2), 1.91 (1H, m, H-4a), 2.13 (1H, m, H-4b), 2.25 (2H, m, H-5), 5.77 (1H, dt, $J=15.4$ and 5.8 Hz, H-6), 5.34 (1H, dd, $J=15.7$ and 10.3 Hz, H-7), 6.00 (1H, dd, $J=10.6$ and 10.6 Hz, H-8), 4.97 (1H, dd, $J=10.6$ and 10.4 Hz, H-9), 2.76 (1H, m, H-10), 1.59 (2H, m, H-11), 1.11 (1H, m, H-12a), 1.83 (1H,m, H-12b), 4.01 (1H, m, H-13), 1.47 (1H, m, H-14a), 1.88 (1H, m, H-14b), 5.03 (1H, brt, $J=$ 3.1 Hz, H-15), 2.22 (2H, m, H-16), 5.30 (1H, d, $J=9.0$ Hz, H-18), 3.39 (1H, dd, $J=12.1$ and 4.0 Hz, H-19a), 3.45 (1H, dd, $J=12.3$ and 9.1 Hz, H-19b), 1.91 (3H, s, H_3-21), 0.98 (3H, d, $J=6.2$ Hz, H_3-22), 3.79 (2H, s, H-2′), 7.21 (1H, d, $J=8.8$ Hz, H-4′), 6.81 (1H, d, $J=$ 8.8 Hz, H-5′), 6.81 (1H, d, $J=8.8$ Hz, H-7′), 7.21 (1H, d, $J=8.8$ Hz, H-8′), 3.77 (3H, s, H-9′), 3.30 ppm (3H, s, O-CH_3); ^{13}C NMR (75 MHz, $CDCl_3$): $\delta=166.3$ (qC, C1), 118.4, (CH, C2), 158.9 (qC, C3), 32.3 (CH_2, C4), 30.9 (CH_2, C5), 131.8 (CH, C6), 125.1 (CH, C7), 127.4 (CH, C8), 136.4 (CH, C9), 29.8 (CH, C10), 31.9 (CH_2, C11), 31.7 (CH_2, C12), 63.0 (CH, C13), 34.7 (CH_2, C14), 66.9 (CH, C15), 33.1 (CH_2, C16), 101.2 (qC, C17), 57.6 (CH, C18), 25.3 (CH_2, C19), 171.4 (qC, C20), 25.2 (CH_3, C21), 21.8 (CH_3, C22), 175.7 (qC, C1′), 42.3 (CH_2, C2′), 126.3 (qC, C3′), 130.8 (CH, C4′), 114.0 (CH, C5′), 159.8 (qC, C6′), 114.0 (CH, C7′), 130.8 (CH, C8′), 55.4 (CH_3, C9′), 48.2 ppm (CH_3, O-CH_3); IR (neat): $\tilde{\nu}_{max}=3693$, 3601, 2928, 2855, 2360, 1694, 1602, 1291, 1090 cm^{-1}; HRMS-ESI: m/z $[M+Na]^+$ calcd for $C_{32}H_{41}NO_7SNa$: 606.2501, found: 606.2500.

***N*-Ethyllatrunculin A (12):** Compound **12** was prepared according to general procedure C starting with **6** (5 mg, 0.011 mmol) in acidic solution (1 mL): 3 h at 60 °C. Elution with *n*-hexane/EtOAc (9:1) afforded **12** (1.3 mg, 26.0%): colorless oil, $[\alpha]_D^{25}=+63.6$ ($c=0.11$ in $CHCl_3$); ^{1}H NMR (400 MHz, $CDCl_3$): $\delta=5.69$ (1H, brs, H-2), 2.64 (1H, m, H-4a), 2.76 (1H, m, H-4b), 2.28 (2H, m, H-5), 5.73 (1H, dt, $J=$ 15.4 and 4.0 Hz, H-6), 6.41 (1H, dd, $J=15.0$ and 11.0 Hz, H-7), 5.97 (1H, dd, $J=10.8$ and 11.0 Hz, H-8), 5.01 (1H, dd, $J=10.4$ and 10.0 Hz, H-9), 2.86 (1H, m, H-10), 1.11 (1H, m, H-11a), 1.76 (1H, m, H-1b), 1.46 (2H, m, H-12), 4.25 (1H, m, H-13), 1.45 (1H, m, H-14a), 1.80 (1H, m, H-14b), 5.44 (1H, brt, $J=3.3$ Hz, H-15), 1.79 (1H, dd, $J=15.4$ and 4.4 Hz, H-16a), 2.14 (1H, m, H-16b), 3.83 (1H, dd, $J=$ 11.7 and 2.2 Hz, H-18), 3.35 (1H, dd, $J=12.1$ and 2.2 Hz, H-19a), 3.49 (1H, dd, $J=12.1$ and 2.6 Hz, H-19b), 1.93 (3H, s, H_3-21), 1.01 (3H, d, $J=6.6$ Hz, H_3-22), 3.45 (1H, dq, $J=17.1$ and 7.0 Hz, H-1′a), 3.76 (dq, $J=17.1$ and 7.0 Hz, H-1′b), 1.18 (3H, t, $J=7.0$ Hz, H-2′), 4.01 ppm (1H, s, OH); ^{13}C NMR (75 MHz, $CDCl_3$): $\delta=167.4$ (qC, C1), 118.0 (CH, C2), 158.7 (qC, C3), 32.7 (CH_2, C4), 30.3 (CH_2, C5), 132.7 (CH, C6), 125.0 (CH, C7), 127.8 (CH, C8), 135.5 (CH, C9), 29.3 (CH, C10), 31.4 (CH_2, C11), 31.3 (CH_2, C12), 63.6 (CH, C13), 35.2 (CH_2, C14), 66.6 (CH, C15), 35.4 (CH_2, C16), 101.0 (qC, C17), 60.5 (CH, C18), 25.4 (CH_2, C19), 173.5 (qC, C20), 25.2 (CH_3, C21), 21.7 (CH_3, C22), 40.6 (CH_2, C1′), 29.9 ppm (CH_3, C2′); IR (neat): $\tilde{\nu}_{max}=3698$, 3606, 3021–2856, 2360, 1660, 1602, 1289, 1089 cm^{-1}; HRMS-ESI: m/z $[M+Na]^+$ calcd for $C_{24}H_{35}NO_5SNa$: 472.2134, found: 472.2133.

***N*-Benzyllatrunculin A (13):** Compound **12** was prepared according to general procedure C from **9** (9 mg, 0.0176 mmol) in acidic solution (1 mL): 5 h at 60 °C. Elution with *n*-hexane/EtOAc (9:1) afforded **12** (1.8 mg, 20.0%): colorless oil, $[\alpha]_D^{25}=+63.6$ ($c=0.17$ in $CHCl_3$); ^{1}H NMR (400 MHz, $CDCl_3$): $\delta=5.68$ (1H, brs, H-2), 1.91 (1H, m, H-4a), 3.38 (1H, dt, $J=13.6$ and 11.0 Hz, H-4b), 2.25 (2H, m, H-5), 5.75 (1H, dt, $J=13.0$ and 5.1 Hz, H-6), 6.36 (1H, dd, $J=15.4$ and 11.0 Hz, H-7), 5.97 (1H, dd, $J=10.8$ and 10.6 Hz, H-8), 5.01 (1H, dd, $J=11.4$ and 10.6 Hz, H-9), 2.90 (1H, m, H-10), 0.89 (1H, m, H-11a), 1.75 (1H, m, H-11b), 1.44 (1H, m, H-12a), 1.67 (1H, m, H-12b), 4.27 (1H, m, H-13), 1.36 (1H, m, H-14a), 1.89 (1H, m, H-14b), 5.42 (1H, brt, $J=3.0$ Hz, H-15), 1.48 (1H, m, H-16a), 2.02 (1H, m, H-16b), 3.88 (1H, dd, $J=9.2$ and 2.9 Hz, H-18), 3.33 (1H, dd, $J=11.0$ and 3.0 Hz, H-19a), 3.66 (1H, dd, $J=11.0$ and 2.6 Hz, H-19b), 1.90 (3H, s, H_3-21), 1.01 (3H, d, $J=6.2$ Hz, H_3-22), 4.43 (1H, d, $J=15.0$ Hz, H-1′a), 5.15 (1H, d, $J=15.0$ Hz, H-1′b), 7.26 (1H, m, H-3′), 7.34 (1H, dd, $J=7.3$ and 1.4 Hz, H-4′), 7.31 (1H, m, H-5′), 7.34 (1H, dd, $J=7.3$ and

1.4 Hz, H-6′), 7.26 (1H, m, H-7′), 3.91 ppm (1H, s, OH); ^{13}C NMR (75 MHz, $CDCl_3$): δ = 166.7 (qC, C1), 117.5 (CH, C2), 158.4 (qC, C3), 32.1 (CH_2, C4), 30.5 (CH_2, C5), 132.0 (CH, C6), 125.0 (CH, C7), 127.7 (CH, C8), 136.4 (CH, C9), 29.3 (CH, C10), 31.7 (CH_2, C11), 30.4 (CH_2, C12), 63.7 (CH, C13), 35.0 (CH_2, C14), 66.9 (CH, C15), 32.7 (CH_2, C16), 101.1 (qC, C17), 62.6 (CH, C18), 27.1 (CH_2, C19), 173.8 (qC, C20), 24.6 (CH_3, C21), 21.7 (CH_3, C22), 48.3 (CH_2, C1′), 136.4 (qC, C2′), 128.2 (CH, C 3′), 128.7 (CH, C4′), 127.4 (CH, C5′), 128.7 (CH, C6′), 128.2 ppm (CH, C7′); IR (neat): $\tilde{\nu}_{max}$ = 3693, 3567, 2996–2855, 2360, 2337, 1663, 1456, 1280, 1091 cm^{-1}; HRMS-ESI: *m/z* $[M+Na]^+$ calcd for $C_{29}H_{37}NO_5SNa$: 534.2290, found: 534.2304.

***N*-Hydroxymethyllatrunculin A (14):** A solution of **1** (10 mg) in EtOH (3 mL) was treated with an aqueous solution of 35% CH_2O (3 mL) and stirred for 24 h at 60 °C.[17] Brine solution (5 mL) was then added, and the mixture was extracted with $CHCl_3$ (2×5 mL). The residue was subjected to chromatography over silica gel 60 using *n*-hexane/EtOAc (8:2) as a solvent system to afford **14** (2.8 mg, 28%): colorless oil, $[\alpha]_D^{25} = +70$ (*c* = 2.2 in $CHCl_3$); ^{1}H NMR (400 MHz, $CDCl_3$): δ = 5.70 (1H, brs, H-2), 2.97 (1H, m, H-4), 2.03 (1H, m, H-5), 5.75 (1H, dt, *J* = 15 and 5.6 Hz, H-6), 6.40 (H1, dd, *J* = 15.5 and 11 Hz, H-7), 5.99 (1H, dd, *J* = 10.8 and 10.6 Hz, H-8), 5.01 (1H, dd, *J* = 10.6 and 10.4 Hz, H-9), 2.71 (1H, m, H-10), 1.05 (1H, m, H-11a), 1.75 (1H, m, H-11b), 1.42 (2H, m, H-12), 4.38 (1H, m, H-13), 1.48 (1H, m, H-14a), 1.72 (1H, m, H-14b), 5.42 (1H, brs, H-15), 1.82 (1H, m, H-16a), 2.05 (1H, m, H-16b), 3.88 (1H, dd, *J* = 7.3 and 7.3 Hz, H-18), 3.33 (1H, dd, *J* = 12 and 9.5 Hz, H-19a), 3.51 (1H, dd, *J* = 12 and 2.6 Hz, H-19b), 1.93 (3H, s, H_3-21), 1.00 (3H, d, *J* = 6.5 Hz, H_3-22), 4.43 (1H, s, C17-OH), 4.65 (1H, dd, *J* = 11.0 and 5.0 Hz, H-1′a), 5.19 (1H, dd, *J* = 11.0 and 9.0 Hz, H-1′b), 3.84 ppm (1H, dd, *J* = 9.0 and 5.0 Hz, CH_2OH); ^{13}C NMR (75 MHz, $CDCl_3$): δ = 165.5 (qC, C1), 117.5 (CH, C2), 158.2 (qC, C3), 32.4 (CH_2, C4), 30.5 (CH_2, C5), 132.0 (CH, C6), 126.1 (CH, C7), 127.3 (CH, C8), 136.3 (CH, C9), 29.2 (CH, C10), 31.8 (CH_2, C11), 31.2 (CH_2, C12), 62.8 (CH, C13), 35.0 (CH_2, C14), 67.9 (CH, C15), 32.1 (CH_2, C16), 98.5 (qC, C17), 66.5 (CH, C18), 28.7 (CH_2, C19), 175.5 (qC, C20), 21.6 (CH_3, C21), 24.5 (CH_3, C22), 68.9 ppm (CH_2, C1′); IR (neat): $\tilde{\nu}_{max}$ = 3400 (br), 2900, 1670.

Biological procedures

Pyrene actin polymerization assays

Actin polymerization assays were carried out as per manufacturer protocols (Cytoskeleton; Denver, CO, USA). Briefly, 5 mM final concentration of monomeric actin (1:10 pyrene labeled) was incubated on ice for 10 min with the indicated concentrations of latrunculin A derivatives. Samples were then equilibrated for 10 min in an ELISA plate reader (BioTek, VT, USA), after which polymerization was induced by the addition of KCl, $MgCl_2$, and ATP. Compounds **1**–**14** were tested at 0.1, 0.5, 1.0, and 10 μM, and IC_{50} values for each compound were calculated using GraphPad Prism version 5.0.

Cell culture

Breast cancer cell lines MCF7 and MDA-MB-231 were purchased from ATCC (Manassas, VA, USA). The cell lines were grown in 10% fetal bovine serum (FBS) and RPMI 1640 (GIBCO-Invitrogen, NY, USA) supplemented with glutamine (2 mmol L^{-1}), penicillin G (100 μg mL^{-1}), and streptomycin (100 μg mL^{-1}) at 37 °C under 5% CO_2.

Preparation of various dilutions of latrunculin A derivatives for cell culture assays

A stock solution of each latrunculin A derivative was prepared by dissolving the compound in DMSO at a concentration of 50 mM for MTT assays and 1 mM for Cultrex assays. About 1 μL of the former solutions was transferred to 999 μL of serum-free medium to obtain 50 μM and 1 μM dilutions (0.001% DMSO) for MTT and Cultrex assays, respectively. Serial dilutions were then conducted to obtain the desired concentrations.

MTT proliferation assays

The growth of MCF7 and MDA-MB-231 cancer cell lines was measured by using an MTT kit (TACS™, Trevigen Inc.).[20,21] Cells in exponential growth were plated in a 96-well plate at a density of 8×10^3 cells per well, and allowed to attach for 24 h. Complete growth medium was then replaced by 100 μL RPMI serum-free medium (GIBCO-Invitrogen, NY, USA) containing various doses (50, 10, 1, 0.5, and 0.1 μM) of the specific tested compound, and culturing was continued at 37 °C under 5% CO_2 for 72 h. The cells were then treated with MTT solution (10 μL per well) at 37 °C for 4 h. The color reaction was stopped by the addition of solubilization/stop solution (100 μL per well), and incubation at 37 °C was continued to ensure complete dissolution of the formazan product. Absorbance of the samples was determined at λ 570 nm with an ELISA plate reader (BioTek, VT, USA). The number of cells per well was calculated against a standard curve prepared by plating various concentrations of cells, as determined by hemocytometer, at the start of each experiment. The IC_{50} value for each compound was calculated by nonlinear regression (curve fit) of log(concentration) versus the number of cells per well, implemented with GraphPad Prism version 5.0 (GraphPad Software, La Jolla, CA, USA).

Cultrex® cell invasion assays

Anti-invasive activities were measured using the Cultrex® cell invasion assay (Trevigen) as previously described.[22,23] About 50 μL of basement membrane extract (BME) coat was added per well. After incubation for 4 h at 37 °C under 5% CO_2, 50000 MDA-MB-231 cells per 50 μL in serum-free RPMI medium were added per well to the top chamber containing the tested compound at the desired concentration (0.1, 0.5, 1 μM). About 150 μL of RPMI medium was added to the lower chamber containing 10% FBS and penicillin/streptomycin with the use of fibronectin (1 μL mL^{-1}) and *N*-formyl-Met-Leu-Phe (10 nM) as chemoattractants. Cells were allowed to migrate to the lower chamber at 37 °C under 5% CO_2. After 24 h, the top and bottom chambers were aspirated and washed with washing buffer supplied with the kit. About 100 μL of cell dissociation dilution/calcein-AM solution was added to the bottom chamber and incubated at 37 °C under 5% CO_2 for 1 h. The cells internalize calcein-AM, and the intracellular esterases cleave the AM moiety to generate free calcein. Fluorescence of the samples was determined at λ_{ex} 485 and λ_{em} 520 nm, with an ELISA plate reader (BioTek, VT, USA). The number of cells that invaded through the BME coat was calculated by a standard curve.

Molecular modeling

Three-dimensional structure building and all modeling were performed with the SYBYL program package,[26] version 8.0, installed on Dell desktop workstations equipped with dual 2.0 GHz Intel® Xeon® processors running the Red Hat Enterprise Linux (version 5) operating system. The X-ray crystal structure of **1** is available,[12]

which provided a template for modeling other latrunculins. To maintain the active conformation, the actin-bound crystallographic structure of **1** was used as template to sketch other derivatives using SYBYL 8.0. Conformations of each compound were generated using Confort™ conformational analysis. Energy minimizations were performed using the Tripos force field with a distance-dependent dielectric and the Powell conjugate gradient algorithm with a convergence criterion of 0.01 kcal mol^{-1} A^{-1}.[27] Partial atomic charges were calculated using the semiempirical program MOPAC 6.0 and applying the AM1 method.[28]

Molecular docking

The SurFlex-Dock program version 2.0 interfaced with SYBYL 8.0 was used to dock the compounds into the active site of actin.[29,30] SurFlex-Dock employs an idealized active site ligand (protomol) as a target to generate putative poses of molecules or molecular fragments.[24,25] These putative poses were scored using the Hammerhead scoring function.[24,25] The program was used to dock the training set molecules into the active site of G-actin. The 3D structure was taken from the RCSB Protein Data Bank (PDB ID: 1ESV).[12]

Acknowledgements

This work was supported by the NIH grant number P20RR16456 from the INBRE Program of the National Center for Research Resources.

Keywords: actin · antitumor agents · cancer · latrunculin A · structure–activity relationships

[1] a) D. J. Newman, G. M. Crag, S. Holbeck, E. A. Sausville, *Curr. Cancer Drug Targets* **2002**, *2*, 279–308; b) J. R. Peterson, T. J. Mitchison, *Chem. Biol.* **2002**, *9*, 1275–1285; c) G. Fenteany, S. Zhu, *Curr. Topics Med. Chem.* **2003**, *3*, 593–616.
[2] a) Y. Kashman, A. Groweiss, U. Shmueli, *Tetrahedron Lett.* **1980**, *21*, 3629—3632; b) A. Groweiss, U. Shmueli, Y. Kashman, *J. Org. Chem.* **1983**, *48*, 3512–3516.
[3] Y. Kashman, A. Groweiss, R. Lidor, D. Blasberger, S. Carmely, *Tetrahedron* **1985**, *41*, 1905–1914.
[4] K. A. El Sayed, D. T. A. Youssef, D. Marchetti, *J. Nat. Prod.* **2006**, *69*, 219–223.
[5] C. Hayot, O. Debeir, P. van Ham, M. van Damme, R. Kiss, C. Decaestecker, *Toxicol. Appl. Pharmacol.* **2006**, *211*, 30–40.
[6] M. Coue, S. L. Brenner, I. Spector, E. D. Korn, *FEBS Lett.* **1987**, *213*, 316–318.
[7] M. Okka, B. Tian, P. L. Kaufman, *Arch. Ophthalmol.* **2004**, *122*, 1482–1488.
[8] P. L. Kaufman, B. Geiger, US Patent 772,412, 2002.
[9] I. Spector, N. R. Shochet, D. Blasberger, Y. Kashman, *Cell Motil. Cytoskeleton* **1989**, *13*, 127–144.
[10] C. Hayot, S. Farinelle, R. De Decker, C. Decaestecker, F. Darro, R. Kiss, M. van Damme, *Int. J. Oncol.* **2002**, *21*, 417–425.
[11] Y. Gashet, S. Tournier, J. A. B. Millar, J. S. A. Hyams, *Nature* **2001**, *412*, 352–355.
[12] W. M. Morton, K. R. Ayscough, P. J. McLaughlin, *Nat. Cell Biol.* **2000**, *2*, 376–378.
[13] M. R. Bubb, L. Govindasamy, E. G. Yarmola, S. M. Vorobiev, S. C. Almo, T. Somasundaram, M. S. Chapman, M. Agbandje-McKenna, R. McKenna, *J. Biol. Chem.* **2002**, *277*, 20999–21006.
[14] K. A. El Sayed, M. A. Khanfar, H. M. Shallal, A. Muralidharan, B. Awate, D. T. A. Youssef, Y. Liu, Y. D. Zhou, D. G. Nagle, S. Shah, *J. Nat. Prod.* **2008**, *71*, 396–402.
[15] T. Amagata, T. A. Johnson, R. H. Cichewicz, K. Tenney, S. L. Mooberry, J. Media, M. Edelstein, F. A. Valeriote, P. Crews, *J. Med. Chem.* **2008**, *51*, 7234–7242.
[16] A. Fürstner, D. Kirk, M. Fenster, C. Aïssa, D. De Souza, C. Nevado, T. Tuttle, W. Thiel, O. Müller, *Chem. Eur. J.* **2007**, *13*, 135–149.
[17] D. Blasberger, S. Carmely, M. Cojocaru, I. Spector, N. R. Shochet, Y. Kashman, *Liebigs Ann. Chem.* **1989**, *12*, 1171–1188.
[18] J. A. Cooper, T. D. Pollard, *Methods Enzymol.* **1982**, *85*, 182–210.
[19] L. Zhai, P. Zhao, A. Panebra, A. L. Guerrerio, S. Khurana, *J. Biol. Chem.* **2001**, *276*, 36163–36167.
[20] T. Mosmann, *J. Immunol. Methods* **1983**, *65*, 55–63.
[21] M. C. Alley, D. A. Scudiero, A. Monks, M. L. Hursey, M. J. Czerwinski, D. L. Fine, B. J. Abbott, J. G. Mayo, R. H. Shoemaker, M. R. Boyd, *Cancer Res.* **1988**, *48*, 589–601.
[22] K. P. Tamilarasan, G. K. Kolluru, M. Rajaram, M. Indhumathy, R. Saranya, S. Chatterjee, *BMC Cell Biol.* **2006**, *7*, 17–30.
[23] P. R. Borghesani, J. M. Peyrin, R. Klein, J. Rubin, A. R. Carter, P. M. Schwartz, A. Luster, G. Corfas, R. A. Segal, *Development* **2002**, *6*, 1435–1442.
[24] W. Welch, J. Ruppert, A. N. Jain, *Chem. Biol.* **1996**, *3*, 449–462.
[25] J. Ruppert, W. Welch, A. N. Jain, *Protein Sci.* **1997**, *6*, 524–533.
[26] SYBYL Molecular Modeling Software, version 8.0, **2007**, Tripos L.P., St. Louis, MO (USA): http://www.tripos.com.
[27] M. Clark, R. D. Cramer III, N. van Opdenbosch, *Comput. Chem.* **1989**, *10*, 982–1012.
[28] J. J. Stewart, *J. Comput. Aided Mol. Des.* **1990**, *4*, 1–105.
[29] E. Kellenberger, J. Rodrigo, P. Muller, D. Rognan, *Proteins Struct. Funct. Bioinf.* **2004**, *57*, 225–242.
[30] A. N. Jain, *J. Med. Chem.* **2003**, *46*, 499–511.

Received: October 15, 2009
Revised: November 17, 2009
Published online on December 30, 2009

